SEMARAK ILMU PUBLISHING

Journal of Advanced Research in Applied Mechanics

Journal homepage:
https://semarakilmu.com.my/journals/index.php/appl_mech/index
ISSN: 2289-7895

Numerical and Experimental Investigation on Aluminium 6061 Solid Cylindrical Bar Subjected to Close-in Blast Loading

Mohd Syedi Imran Mohd Dawi[1,*], Ahmad Humaizi Hilmi[1], Muhamad Saifuldin Abdul Manan[1], Ahmad Mujahid Ahmad Zaidi[2], Mohd Sabri Hussin[1], Perk Lin Chong[3]

[1] Faculty of Mechanical Engineering and Technology, Universiti Malaysia Perlis, Malaysia
[2] Faculty of Engineering, National Defence University of Malaysia, Malaysia
[3] Centre for Sustainable Engineering, School, of Computing, Engineering & Digital Technologies Engineering, Teesside University, United Kingdom

ARTICLE INFO

Article history:
Received 24 September 2023
Received in revised form 26 November 2023
Accepted 14 December 2023
Available online 15 January 2024

Keywords:
ABAQUS simulation; Aluminum 6061; close-in blast load; deformation behaviour; explosive compaction

ABSTRACT

Compaction force generated by blasting load requires strong material such as steel to act as a plunger to spread the force evenly. The problem with this method is retaining the plunger's original dimension from intolerable deformation. This paper uses ABAQUS software to study the ability to predict the response of solid cylindrical aluminium bars (6061) subjected to different close-in blast loads. The solid cylindrical aluminium bars treated as a plunger were evaluated numerically using a combination of the finite element method (FEM) and smoothed particle hydrodynamic (SPH) methods. The plunger was simulated using the Johnson-Cook (J.C.) model, and Jones-Wilkins-Lee (JWL) equation parameters modelled the explosive. Field tests were conducted by detonating explosives of two different weights, which are 100g and 250g, in the designated blast area. Both data and observation were compared and analysed regarding deformation behaviour in term of dimension difference and fracture. Based on the graph of the deformation dimension versus the plunger length, the deformation trend shows a very close relation between numerical and experimental data with a percentage error of less than 4%. The fracture mode generated using FEM is comparable to the actual specimen. This fracture mode can be described as similar to the behaviour of the specimen obtained using the Taylor impact test. Thus, it can be concluded that the numerical analysis performed for this study is consistent with the actual results.

1. Introduction

Explosives are widely recognised for their capacity to generate destructive and life-threatening force. Beyond their application in the defence industry, the instantaneous release of mass energy in an explosion has demonstrated its utility in various civil engineering applications, including quarrying, building demolition, and specialised manufacturing techniques like explosives welding. Numerous additional studies also have been conducted to exploit the results of explosions for product development. One of the research focuses is on the capability of utilising explosive energy as a

* *Corresponding author.*
E-mail address: syediimran@unimap.edu.my

https://doi.org/10.37934/aram.113.1.138151

substitute for conventional compaction and compression processes. Explosive compaction, also known as explosive compression, is used in various fields, such as structural engineering, geotechnical engineering, and materials science [1]. It involves using explosives to compact or compress materials, resulting in increased density or improved mechanical properties. Materials science research has explored the fabrication of composite metals using explosive compaction techniques [2]. The method allows the production of specimens with a constant cross-section over several meters. Yuan *et al*., [3] studied the cylinder test of aluminised explosives with different content of Al powder. They investigated the accelerating ability of explosives based on cyclotetramethylenetetranitramine (HMX) and different sizes of Al or lithium fluoride (LiF) powder. The research provides insights into the effect of Al powder content on the performance of aluminised explosives.

All the previous studies generally consist of explosive material and specimen containers such as cavity mould or base plates for momentum traps. The explosive was situated at varying distances from the target material. However, some researchers use intermediate materials such as water [4] or steel plug [5]. Intermediate materials are extremely important in explosive compaction operations. They provide a variety of purposes, including shockwave control, which ensures that the intense shockwaves produced during compaction do not cause excessive damage to the target material, allowing consistent compaction. These materials also serve as confinement layers, containing and directing the explosive power exactly toward the target material to guarantee successful compaction. Furthermore, some intermediate materials are intended to improve the compaction process by increasing energy transmission from the explosive charge to the target material, thus resulting in improved compaction.

This research aims to study blast load experiments further to develop a compaction or compression method that can be integrated into manufacturing processes. The initial study begins by understanding the pressure forces generated within a closed container due to explosive forces [6]. Subsequently, further research is conducted to test the design capabilities of a device in compressing metal [7]. A similar device design is also used to create a green compact iron powder for the powder metallurgy [8]. These tests related to compression and compaction share a common feature, which is the use of a metal cylinder as an intermediate material between the specimen and the explosion. A cylindrical metal, called a plunger, is adapted from the conventional method in the metal powder compaction process [9, 10]. While the explosive detonates, it generates a blast load transmitted via the metal plunger to the targeted specimen. The used steel as the plunger spreads the compaction force more evenly, resulting in a more consistent shape or surface for the specimen.

The problem with this method is that the success of the experiment depends on the geometry, dimension, and plunger material. The plunger's capacity to retain its shape following an explosion reflects its ability to feed energy efficiently (minimum energy lost in the form of deformation or fragment). The top surface deformation (where the blast load meets the plunger) and bottom surface deformation (where the plunger is designed to impact another material to be compressed or compacted) are failure criteria in these experiments. When there is significant deformation on the top of the plunger, it cannot be used again. However, the possibility of minor deformation allows for repeated use. This is not the case with the bottom surface, where the plunger's shape must remain consistent with the design, as it will imprint on the material if deformed. In contrast to stand-off operations, where there is typically a distance or intermediary material between the blast and the test specimen, very few close-in blast load tests have been conducted. Close-in refers to an explosion that occurs at a very close distance; in this scenario, the explosive is set directly on one surface of the specimen.

It is critical to anticipate the degree of plunger failure. Once the experiment is detonated, failure results in a loss of time and resources for the researcher. Regardless of whether the specimen obtained is as planned, these experiments need months of detailed planning before implementation. Thus, this study aims to investigate the response of a plunger subjected to a close-in blast load. The research focuses on verifying the accuracy of numerical analysis as a predictive technique for evaluating material deformation and fracture. An aluminium 6061 cylindrical bar alloy was used as a plunger and subjected to two different blast load conditions.

Numerical simulations such as the finite element technique (FEM) and the boundary element method (BEM) have been extensively employed for this purpose [11]. The detonation of an explosion can be accurately represented using a set of constants, which includes the Jones-Wilkins-Lee (JWL) equation parameters and the C-J parameters for the explosives [12]. It is implemented as a material model in various dynamic modeling software programs such as ABAQUS, LS-DYNA, AUTODYN, and others. ABAQUS and ANSYS are widely utilized software tools for conducting dynamic simulations. Various studies have been conducted to compare these two platforms, revealing minimal differences in their outcomes [13].

In conclusion, several experimental studies utilise explosives and metals as intermediates to produce specific products. However, there is a notable lack of literature that explicitly investigates these intermediate materials' properties. More critically, these detonations occur in direct contact with the explosive material. This study focuses on the effects of the explosion on a metal plunger in terms of deformation and failure behaviour, as well as the computer simulation's capability to predict these effects. This research is instrumental in the design phase of the future devices.

2. Methodology

The blast loading test was conducted using a cylindrical bar 6061 aluminium alloy called a plunger, where the cylinder shape charge with controlled weight is detonated right on the top end while another end is rested on a steel base plate. The 6061 aluminium is chosen due to its lower yield strength compared to steel. Additionally, it benefits by lowering the cost and difficulty scale of the experimental process by utilising the smallest amount of explosive material possible for the material to deform or fail. The dimensions of the aluminium plunger are approximately 50.8 mm in diameter and 180 mm in length. The weight is close to 1000 grams (refer to Table 1). There are two sets of experimental setups with two different explosive weights. The selection of a 250 g charge weight was intentional to deliberately fracture the plunger, whereas opting for a 100 g charge weight was made with the objective of causing deformation in the explosion without significantly fragmenting the plunger.

Table 1
Experimental parameter

Item	Actual (Diameter × length)	Weight (gram)	Charge weight (gram)
A	50.9 mm × 180.27 mm	985	100
B	50.9 mm × 180.42 mm	984	250

2.1 Computational Model

A numerical simulation was completed before conducting the experiment to predict the plunger's deformation and change in dimension. The flow chart for the numerical simulation technique is depicted in Figure 1. The FE code used to conduct the numerical simulations for this study is ABAQUS/Explicit.

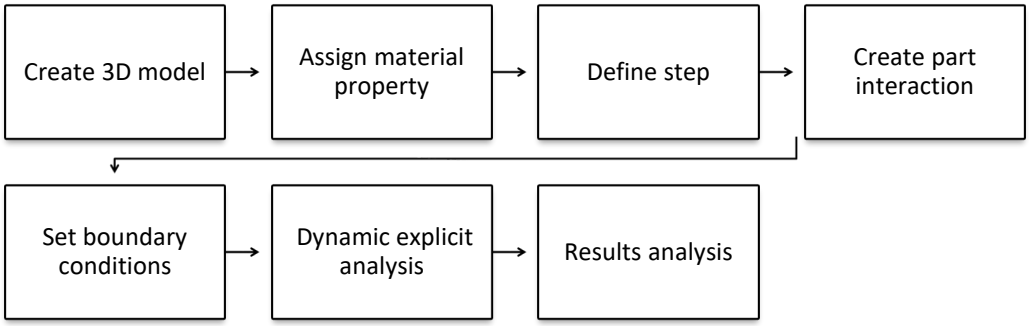

Fig. 1. General flow for the numerical study

This work has utilised the ABAQUS/Explicit FE code, enabling the anticipation of outcomes in a high-speed blast-loading experiment. Shear cracking and fragmentation, which are not axially symmetric, have been observed at the impact end of the blast loading. These phenomena cannot be predicted using an axially symmetric finite element model. Therefore, a three-dimensional FE model has been constructed. The shape used for 100 g of explosives is a cylinder with a diameter of 50 mm and a height of 42.44 mm. For 250 g of explosives, the height used is 106.10 mm. The plunger specimen is a cylinder with a diameter of 50.8 mm and a height of 180 mm.

The technique of element removal is used to replicate the initiation and spread of cracks. The procedure for eliminating elements is a way to get the required material separation outcome, and this method results in a loss of mass, momentum, energy, et cetera. Therefore, elements in the probable fracture region should be kept small enough to minimise the effects of element removal on the impact response. This should be accomplished while keeping the computational expense manageable. Figure 2 shows the FEM modelling of the explosive, specimen, and base plate meshed by eight-node, linear brick elements with C3D8R element. Each part rests on top of the other with no gap between them. As depicted in Figure 2(a), the base plate's bottom surface is fixed to resemble the true boundary conditions. In order to set the position, boundary conditions of the encastre (U1=U2=U3=UR1=UR2=UR3 = 0) were applied to the base plate's bottom surface. The general contact interaction was applied to all models. The number of elements for specimen A, explosive, and base plate is 182400, 206304, and 1875, respectively. In comparison, specimen B is 196800, 260336, and 1875 elements. Structured mesh (Figure 2(b)) was used and as seen in Figure 2(c), very fine meshes were generated at one end which is directly exposed to blast impact. Its length is 20 mm long, where fracture may develop for 100 gram explosive blast, and 60 mm long for 250 gram, while relatively coarse meshes were used in the rare part of the specimen and also for the base plate. The minimum element size is 1 mm, and the maximum is 3 mm for the specimen. While element size for explosives and base plate is consistent across parts which are 1 mm and 8 mm, respectively. As for explosives, the element type is converted to a particle, known as the SPH method. The explosive part was initially set as a structured mesh for accuracy [14]. For this study, the finest size of the SPH element is set at 1 mm due to limitation of the computer hardware capacity to perform the analysis within an acceptable time frame without compromising the quality of results. As example, Figure 3 is made to show the results of specimen A obtained with a 1.0 mm explosive mesh size were compared side by side with those of a 0.5 mm mesh size, which was later converted to SPH elements. It was observed that the computational time increased by a factor of 15, and the results did not correlate well with the experimental data. However, SPH is a mesh-free technique [15] ideally suited to simulate complex boundary dynamics such as explosive blast tests. Numerous previous studies have demonstrated that this method is more realistic than other tested methods specifically for blast load

analysis [16,17]. Some researchers use the same method for high-impact damage and have the same conclusion [17–19]. The detonation point is set near the explosive model at the top surface.

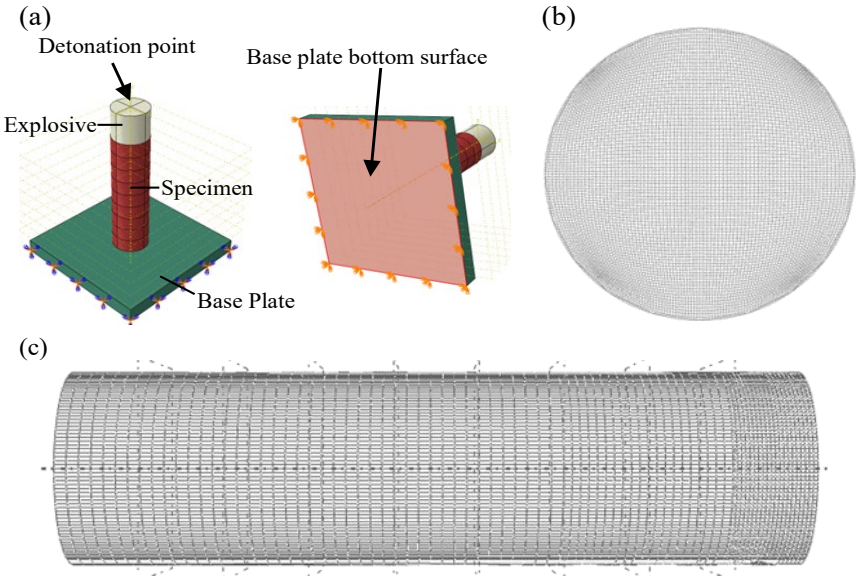

Fig. 2. FEM modeling of the blast loading test: (a) Experiment model (b) mesh of the specimen cross-section (c) mesh of the specimen section plane

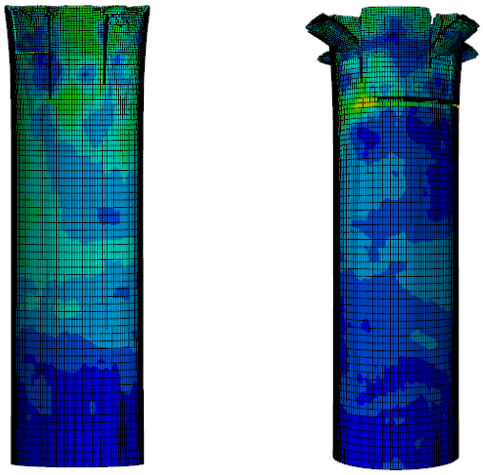

(a) (b)

Fig. 3. The example of comparison between 1mm mesh size (a) and 0.5mm mesh size (b) result for specimen A

The 6061 aluminium was modelled using the Johnson-Cook (JC) plasticity and damage model. It is typically combined with the Johnson-Cook plasticity model to comprehensively represent material response under impact. The JC plasticity model characterised the plastic behaviour of the plunger under high strain rates and elevated temperatures. The formula is given as shown in Eq. (1) below:

$$\sigma = (A + B\varepsilon^{n})(1 + C\ln\dot{\varepsilon}^{*})(1 - T^{*m}) \quad (1)$$

where σ is the equivalent stress; A is the yield stress of the material under reference conditions; B is the strain hardening constant; n is the strain hardening coefficient; ε is the strain; C is the strengthening coefficient of strain rate; $\dot{\varepsilon}^*$ is the strain rate; T is the temperature, and m is the thermal softening coefficient.

Conversely, the JC damage model is often used to predict material failure and damage evolution in dynamic loading conditions. The damage model is formulated in its general form as shown in Eq. (2) below [21]:

$$\varepsilon_f = [D_1 + D_2 \exp(D_3\sigma^*)](1 + D_4 \ln \dot{\varepsilon}^*)(1 + D_5 T^*) \quad (2)$$

where D_1, D_2, D_3, D_4, D_5 are material constant. Other parameters have the same meaning as in the plasticity model. The JC constants have been applied for this study and are presented in Table 2 [22]. The tensile strength was set at 332 MPa as the tensile failure value [23].

The JWL equation of state has been used in this explosive model due to its simplicity in hydrodynamic calculations and its tendency to generally produce accurate results compared to experimental tests as shown in general form in Eq. (3) below:

$$p = A\left(1 - \frac{\omega}{R_1 v}\right)e^{-R_1 v} + B\left(1 - \frac{\omega}{R_2 v}\right)e^{-R_2 v} + \frac{\omega E}{v} \quad (3)$$

where A, B, R_1, R_2, and ω are parameters; p is the pressure; e is the specific internal energy, and v is the relative volume. Two types of explosive weight were modelled, and the JWL parameter was identified and entered for computer simulation as in Table 3 [24,25]. In addition, the interaction between the parts is set as general contact.

Table 2
J.C. parameter for 6061-t6 aluminum

E MPa	*v*	A MPa	B MPa	n	C	M
6.9e4	.33	324	114	.42	.002	1.34
D_1	D_2	D_3	D_4	D_5	T_{melt} K	T_{room} K
-.77	1.45	-.47	0	1.60	650	293.15

Table 3
JWL (EOS) of explosives

ρ Tonne/mm^3	VOD mm/s	A MPa	B MPa	C MPa	R_1	R_2	E_0 MPa	ω
1.2e-9	3.5e6	209685	3509	517	5.762	1.290	2386	0.39

ρ: Density; VOD: Velocity of detonation; A, B,C,R1,R2, E0 and ω :JWL constant.

2.2 Blast Loading Experiment

The blast field was constructed at the quarry site. The experiment was set up as depicted in Figure 4, including its several components listed in Table 4.

Table 4
Components

No.	Component
1	Electric detonator
2	Explosive (emulsion explosive)
3	PVC casing
4	Aluminum Plunger (specimen)
5	Base Plate (momentum trap)

Several holes roughly 4 feet deep were prepared with an excavator prior to blast test setup. Another hole was dug at one side of the wall to accommodate the specimen arrangement (Figure 4 and Figure 5a). This arrangement was made for safety and served as a trap for specimens exhibiting the rebound phenomenon.

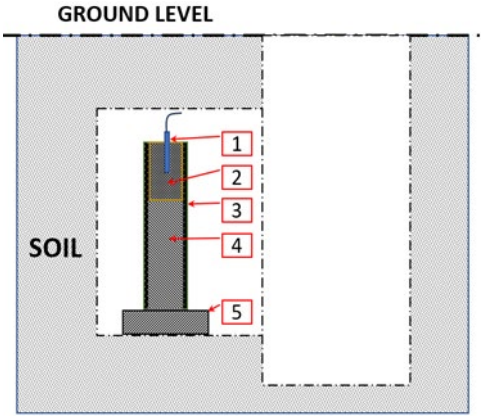

Fig. 4. Experimental setup

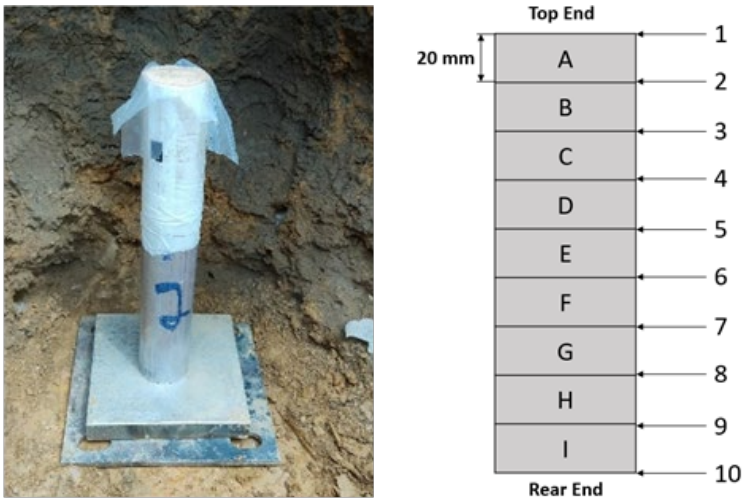

Fig. 5. (a) Specimen set up (b) Plunger's segmented diagram

Aluminium 6061 plungers are individually blasted with two different explosive weights, resulting in two different blast loads. The changes in shape and dimensions of the specimens are recorded. After the blast experiment, the plunger's length, diameter, and overall shape are recorded and observed. Each plunger is segmented into nine sections to facilitate accurate and systematic dimensioning (as shown in Figure 5b). The diameter at different locations (numbers 1-10) and length (alphabetical A-I) of each segment were measured using the vernier calliper in this investigation. This division is made to monitor deformation occurring along different portions of the plunger. The choice

of 20 mm is made for ease of measurement, as smaller measurements can be challenging when the region is in close proximity to the point of detonation. Therefore, a length of 20 mm is considered adequate for this study. Based on the dimension measured after the experiment, the percentage of error was calculated, and a graph was generated to illustrate the deformation trend between the two results and the degree to which the predicted outcome matches the actual result. The experimental result was validated by comparing it to numerical simulation results.

3. Experimental Results: Validation and Verification

Numerical simulation results of the aluminium plunger are compared to experimental results. Figure 6 shows the visualisation from computer simulation for the actual state of both specimens following the explosion. Firstly, the severity of plunger deformation is compared. For a 100g charge weight (Figure 6a), the modelling forecasts a mushroom shape distortion with cracks, but a 250g charge weight results in severe deformation and material separation (Figure 6b). The material fragments are blown away, reducing the weight of the plunger. The same incident goes with the experimental plunger. Specimen A weighs 985g before the blast and reduces to 983g after the blast. As for specimen B, it weighs 984g before the blast and becomes 795g afterwards. While the weight of the specimens after the blast, according to simulation, is 960g for specimen A and 650g for specimen B. In terms of weight difference, specimen A has a percentage error of 2.3%, while specimen B has 22.3%. A higher percentage error for specimen B is due to the simulation predicting that almost half of the plunger will be entirely detached, which has not occurred in the actual specimen. Although the degree of damage to almost one-third of the plunger was also demonstrated experimentally, some material remains attached to the main body despite the severe deformation. Thus, the damage prediction is acceptable, as both conditions are heavily damaged.

The results of vertical or lengthwise and horizontal or radial deformation observations were also recorded and analysed. The comparison of simulation results and explosion experiment results for specimen A demonstrates that it is consistent with the simulation results, where the percentage error for total length is 0.15%. Percentage error for each segment length ranges between 0% and 17%, with an average of 3.86%. While the percentage error of diameter varies between 0.21% and 13.13%, with an average of 2.22%. The data for specimen B also shows an acceptable result as specimen A. The percentage error of the length ranges from 0.9% to 3.5%, with an average of 1.9% for each segment. The percentage error of the total length is calculated as 19.44%. The high percentage of total length is due to the simulated data for the plunger losing its material being not accurately the same (as clarified earlier). In terms of diameter, the range is between 0.03% and 0.31%, with an average of 0.19%.

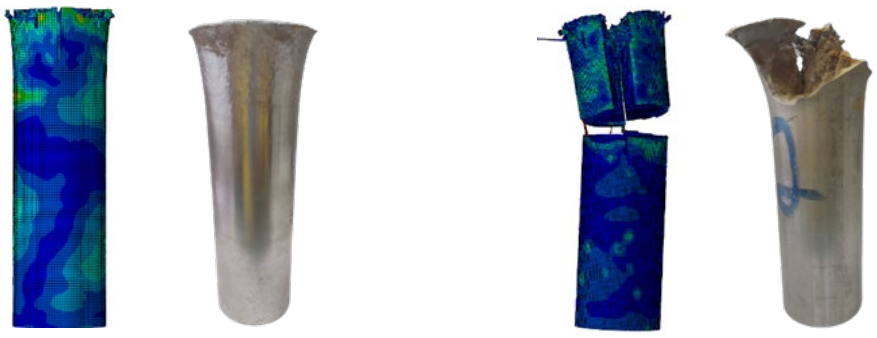

(a) (b)

Fig. 6. Visualisation of simulation and experimental specimen (a) 100 gram explosive (b) 250 gram explosive

Figure 7 represents the length of each segment as measured and compared to the overall length of the plunger, where the first point belongs to the first segment where it meets the blast force. Each line has 9 points representing A-I segments, as described in Figure 5(b). The graph illustrates the large difference in dimension between the initial (measurement before the blast test) and the final value for both data from the experiment and simulation, notably in the first segment. The graph also indicates that the length reduction of segments decreases with increasing distance from the blast point. In terms of the change in the physical shape of the plunger following the blast, the average length difference is less than 1 mm and has no significant effect. The decrease in length of the bottom end of the segment is negligible. Overall, the simulation's deformation trend is consistent with the experimental result.

The same pattern can also be found in Figure 8, which examines the changes in the radial dimension. Each point represents locations 1 to 10 (see Figure 5(b)), where the diameter of the plunger was measured. Similarly, the specimen's top end surface exhibited a rather significant diameter change. As it moves farther away from the source of the explosion, the change in diameter decreases. When analysing simulation and experimental data, it is clear that the discrepancy in results between points 1 and 2 is relatively considerable. In this instance, distance to the blast origin may play a major role. However, this difference gap narrows after the third point, when the simulation can predict nearly identical results to the experiment.

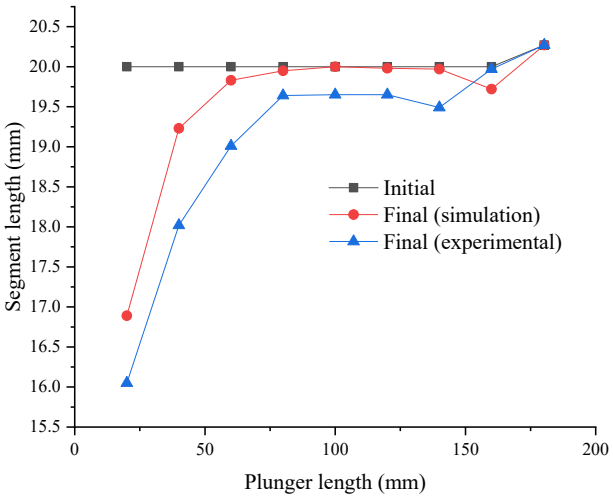

Fig. 7. Segment length deformation n vs Plunger length for A specimen

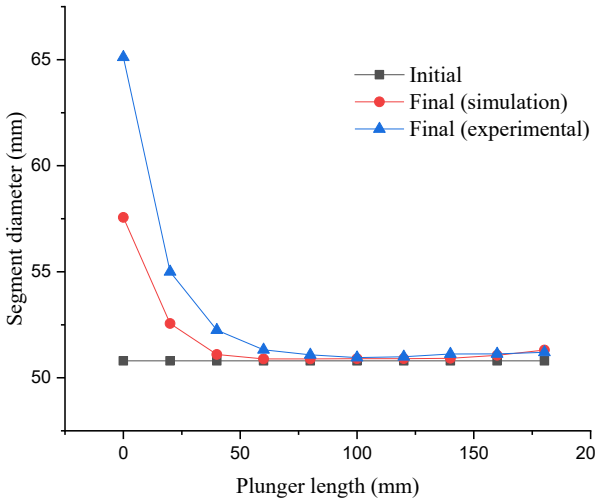

Fig. 8. Segment diameter deformation vs Plunger length for specimen A

As for specimen B, the absence of data indicates that the plunger condition is not measurable at that segment. The specimen's material was separated upon blast loading. Compared to the graph for specimen A, the overall accuracy of the prediction for specimen B shown in Figure 9 is relatively low. This is evident in the experimental line trend, where the first three points cannot be observed due to the breakage of the top three segments. The simulation however predicted that the top five segments would shatter due to the blast. From a different perspective, the simulation has accurately predicted the extent of plunger fracture despite being less precise. The final segment's measurements are also extremely close to the experimental results. As a result of damage to a portion of the plunger, the same condition applies to Figure 10 when simulation and experiment data are restricted to the remaining material. The rest of the existing data shows a relatively good correlation. The disparity between simulation and experimental data is less than 1 mm.

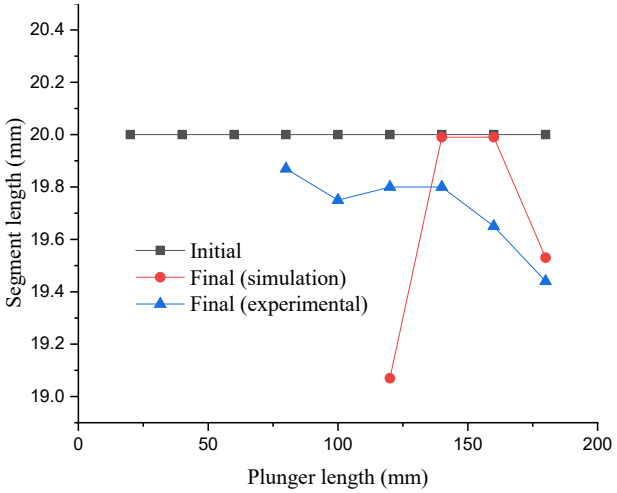

Fig. 9 Segment length deformation vs Plunger length for specimen B

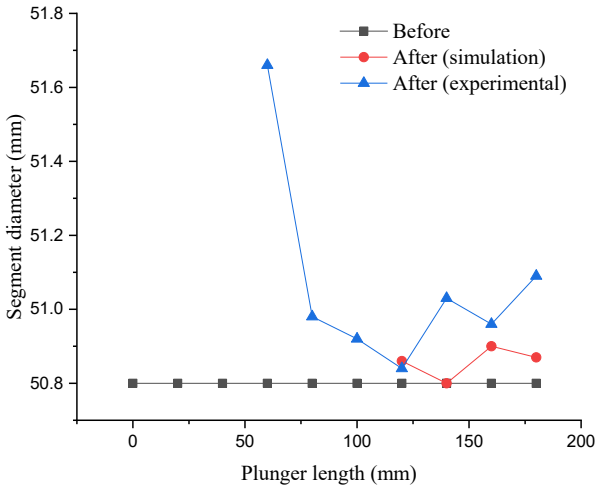

Fig. 10. Segment diameter deformation vs Plunger length for specimen B

4. Results and Discussion

This section provides a summary of the findings of the blast loading study. By measuring the deformed specimens created by computer simulation, the behaviour of the aluminium material at different charge weights could be observed.

Deformation behaviour based on a 100g (specimen A) explosive load is comparable to the Taylor impact test experiment [26,27], with the exception that the Taylor test required the cylindrical specimen to impact on a rigid plate at high speed, causing deformation. Depending on the material's properties and velocity, the specimen may retain its original form, become deformed, or fracture. While in this study, a cylindrical specimen was used in which one surface rests on a rigid plate and another end is directly in contact with explosive material. The generated blasting load at the surface directly in contact with the explosion will have a similar force effect as the force generated by the projectile impact of a rigid body. In the event of an explosion, elastic waves and plastic waves are produced at the impact interface direction. Since a base plate (momentum trap) stops the specimen from moving downward, the top part of the cylinder bulges out and deforms in the radial direction. The rear part however deformed at a very minimum value. The overall length is decreased due to impact load. After the plastic deformation and elastic behaviour of the specimen have absorbed the blast loading, the specimen will begin to rebound as it was retrieved further away from the base plate.

This study reveals the deformation behaviour can be categorised as tensile splitting/petalling as demonstrated in the Taylor impact test. Although Taylor mushrooming can be seen obviously for specimen A, further inspection shows several cracks occurred at the edge of the surface as shown in Figure 11. Closed observation on the surface shows the crack direction is along the axis of explosive impact for cylinder shape charge where the explosion direction is moving away from detonator towards the specimen surface. The simulation also predicted the same crack behaviour as shown in Figure 12. The surface's diameter has expanded to 65.12 mm or a 27.9% increase. While simulation predicted the diameter to reach 57.56 mm or a 13.3% increase. The rear surface diameter however reached 51.13 mm, or a 2.1% increase and simulations predicted 51.06 mm or a 0.5% increase.

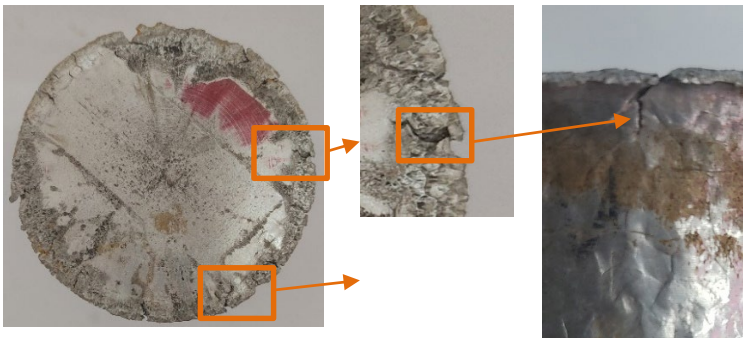

Fig. 11. Cracking discovered on specimen A surface for 100 gram explosives

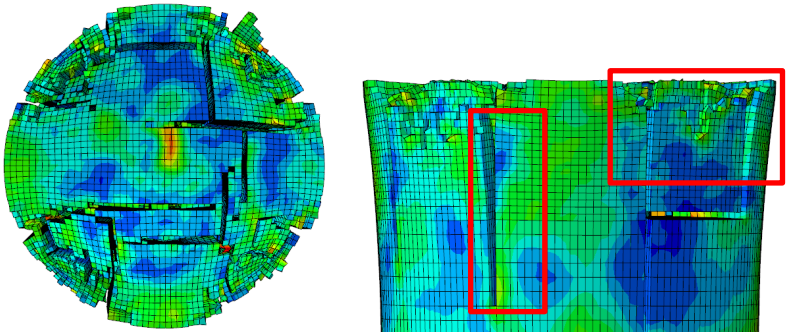

Fig. 12. Critical cracking as predicted in simulation for specimen A

As for the 250g explosive load, the specimen's top surface was fractured due to explosive impact. The added weight of explosive material increases the impact and causes the top end to be shattered into fragments. Figure 13 shows recovered specimen B, and its fragments. Distinct from specimen A, the blast surface of specimen B was fractured and broke off. The specimen condition is also similar to Taylor impact research regarding 7404 aluminium [26] which the failure can be concluded due to the shear crack that extended along the specimen and subsequently caused the fragmentation. Even though there is a slight difference in fragment size due to the different impact force and material (aluminium 6061) simulated in this study, the causes of the deformation and fracture modes of shear cracking and fragmentation that occurred in specimen B are the same. The condition of high shear stress causes the material to be fractured. The simulation visualisation reveals that the material is separated by up to 60 mm from the top end (Figure 14), while experimentation indicates that the material is separated up to 50 mm from the top end.

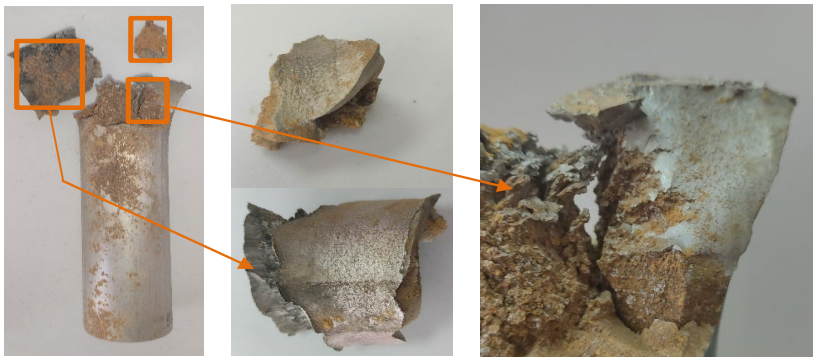

Fig. 13. Shattered fragments and large cracking discovered in specimen B

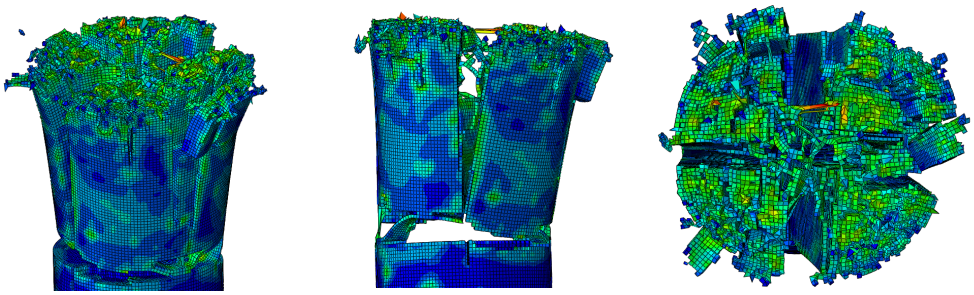

Fig. 14. Moment before specimen fragments flew off

5. Conclusions

In conclusion, this study investigated the deformation behaviour of aluminium 6061 plungers subjected to different explosive loads through numerical simulations and experimental tests. The numerical simulation results were compared to the experimental data, and the findings are as follows:

i. The simulation accurately predicted the severity of plunger deformation for both 100g and 250g charge weights. For the 100g charge weight, the modelling forecasted a mushroom shape distortion with cracks, while the 250g charge weight resulted in severe deformation and material separation. The experimental and simulated weight reductions of the plungers were consistent, demonstrating acceptable damage prediction.

ii. The comparison between simulation and experimental results for specimen A showed close agreement, with percentage errors ranging between 0% and 17% for segment lengths and between 0.03% and 13.13% for diameter. Specimen B, which experienced severe fragmentation, exhibited higher percentage of errors due to the challenge in accurately predicting detachment points. The simulation demonstrated consistent deformation trends with experimental results for both lengthwise and radial dimensions. The length reduction of segments decreased with increasing distance from the blast point, and the change in diameter decreased as the measurement moved farther away from the explosion source.

iii. Specimen A displayed tensile splitting/petalling behavior, similar to the Taylor impact test. Cracks appeared along the axis of the explosive impact, and the surface diameter increased in both the experimental and simulation results. Specimen B exhibited more severe fragmentation, with the top surface being fractured and broken off. The simulation correctly predicted the shear cracking and fragmentation modes responsible for the material's separation.

Overall, the numerical simulation results were in good agreement with the experimental data, demonstrating the effectiveness of the ABAQUS/Explicit FE code in predicting the behaviour of aluminium 6061 plungers under blast loading. The study provides valuable insights into the deformation and fracture characteristics of the plungers, offering essential information for blast load analysis and structural design. The investigation also successfully predicted the degree of plunger deformation and failure, aligning well with the experimental observations and exhibiting comparable fracture modes to the Taylor impact test experiment. The deformation trends with different blast loads were depicted through deformation-segment traces, displaying a consistent pattern. This established computer numerical analysis is highly reliable with tolerable percentage errors, and the collated data serves as a valuable resource for future reference and understanding.

Acknowledgement
This research is fully supported by Fundamental Research Grant Scheme (FRGS), FRGS/1/2018/TK03/UNIMAP/02/21. The authors express their gratitude to the Ministry of Higher Education (MOHE) and Universiti Malaysia Perlis for approving funds that enabled this critical research to be viable and effective.

References

[1] Lukić, Sanja, and Hrvoje Draganić. "Blast Loaded Columns—State of the Art Review." *Applied Sciences* 11, no. 17 (2021): 7980. https://doi.org/10.3390/app11177980
[2] Nishi, Masatoshi, Shigeru Tanaka, Matej Vesenjak, Zoran Ren, and Kazuyuki Hokamoto. "Fabrication of Composite Unidirectional Cellular Metals by Using Explosive Compaction." *Metals* 10, no. 2 (2020): 193. https://doi.org/10.3390/met10020193
[3] Yuan, Xiaoxia, Hongliang Ma, Lei Zhang, and Fang Li. "Study on the cylinder test of aluminized explosives with different content of Al powder." In *Journal of Physics: Conference Series*, vol. 2478, no. 3, p. 032019. IOP Publishing, 2023. https://doi.org/10.1088/1742-6596/2478/3/032019
[4] Zohoor, M., and A. Mehdipoor. "Explosive compaction of tungsten powder using a converging underwater shock wave." *Journal of materials processing technology* 209, no. 8 (2009): 4201-4206. https://doi.org/10.1016/j.jmatprotec.2008.11.031
[5] Sivakumar, K., T. Balakrishna Bhat, and P. Ramakrishnan. "Effect of process parameters on the densification of 2124 Al–20 vol.% SiCp composites fabricated by explosive compaction." *Journal of materials processing technology* 73, no. 1-3 (1998): 268-275. https://doi.org/10.1016/S0924-0136(97)00237-9
[6] Hilmi, Ahmad Humaizi, Nor Azmaliana Azmi, and Ariffin Ismail. "A method to press powder at 6000 ton using small amount of explosive." In *AIP Conference Proceedings*, vol. 1901, no. 1. AIP Publishing, 2017. https://doi.org/10.1063/1.5010494
[7] Azmi, Nor Azmaliana, Ahmad Humaizi Hilmi, M. Alias Yusof, and Ariffin Ismail. "Characteristic of Solid Metal using Underground Explosion Pressing." In *IOP Conference Series: Materials Science and Engineering*, vol. 429, no. 1, p. 012096. IOP Publishing, 2018. https://doi.org/10.1088/1757-899X/429/1/012096
[8] Azmi, Nor Azmaliana, Ahmad Humaizi Hilmi, M. Alias Yusof, and Ariffin Ismail. "Characteristics of Iron powder when Pressed using Explosive Pressing method." In *IOP Conference Series: Materials Science and Engineering*, vol. 429, no. 1, p. 012095. IOP Publishing, 2018. https://doi.org/10.1088/1757-899X/429/1/012095
[9] Tuo, Chengjiong, Zhenhua Yao, Wei Liu, Shengfa Liu, Li Liu, Zhiwen Chen, Shangyu Huang, Changqing Liu, and Xueqiang Cao. "Fabrication and characteristics of Cu@ Ag composite solder preform by electromagnetic compaction for power electronics." *Journal of Materials Processing Technology* 292 (2021): 117056. https://doi.org/10.1016/j.jmatprotec.2021.117056
[10] Ammar, Hany R., S. Sivasankaran, Abdulaziz S. Alaboodi, Yaser A. Alshataif, and Fahad A. Al-Mufadi. "Synthesis, phase evolutions, microstructures, and compaction behavior of four copper-chalcogenide micron-thermoelectric powders (Cu2ZnSnS4/Se4, Cu2MnSiS4/Se4, Cu2MnSnS4/Se4, and Cu2ZnSiS4/Se4) prepared by mechanical alloying." *Materials Chemistry and Physics* 271 (2021): 124943. https://doi.org/10.1016/j.matchemphys.2021.124943
[11] Yamamoto, Isamu, Tomohiko Mukaiyama, Katsunori Yamashita, and ZhengMing Sun. "Effect of loading rate on absorbed energy and fracture surface deformation in a 6061-T651 aluminum alloy." *Engineering Fracture Mechanics* 71, no. 9-10 (2004): 1255-1271. https://doi.org/10.1016/S0013-7944(03)00241-8
[12] Castedo, R., M. Natale, L. M. López, J. A. Sanchidrián, A. P. Santos, J. Navarro, and P. Segarra. "Estimation of Jones-Wilkins-Lee parameters of emulsion explosives using cylinder tests and their numerical validation." *International Journal of Rock Mechanics and Mining Sciences* 112 (2018): 290-301. https://doi.org/10.1016/j.ijrmms.2018.10.027
[13] Quanjin, Ma, M. N. M. Merzuki, M. R. M. Rejab, M. S. M. Sani, and Bo Zhang. "Numerical Investigation on Free Vibration Analysis of Kevlar/Glass/Epoxy Resin Hybrid Composite Laminates." *Malaysian Journal on Composites Science & Manufacturing* 9, no. 1 (2022): 11-21. https://doi.org/10.37934/mjcsm.9.1.1121
[14] Blacker, T. "Automated conformal hexahedral meshing constraints, challenges and opportunities." *Engineering with Computers* 17 (2001): 201-210. https://doi.org/10.1007/PL00013384
[15] Liu, M. B., G. R. Liu, and Z. Zong. "An overview on smoothed particle hydrodynamics." *International Journal of Computational Methods* 5, no. 01 (2008): 135-188. https://doi.org/10.1142/S021987620800142X
[16] Liu, M. B., G. R. Liu, Z. Zong, and K. Y. Lam. "Computer simulation of high explosive explosion using smoothed particle hydrodynamics methodology." *Computers & Fluids* 32, no. 3 (2003): 305-322. https://doi.org/10.1016/S0045-7930(01)00105-0

[17] Karmakar, Somnath, and Amit Shaw. "Response of RC plates under blast loading using FEM-SPH coupled method." *Engineering Failure Analysis* 125 (2021): 105409. https://doi.org/10.1016/j.engfailanal.2021.105409
[18] Mardalizad, Aria, Timo Saksala, Andrea Manes, and Marco Giglio. "Numerical modeling of the tool-rock penetration process using FEM coupled with SPH technique." *Journal of Petroleum Science and Engineering* 189 (2020): 107008. https://doi.org/10.1016/j.petrol.2020.107008
[19] Zhong, Hanqing, Liang Lyu, Zhixiang Yu, and Chun Liu. "Study on mechanical behavior of rockfall impacts on a shed slab based on experiment and SPH–FEM coupled method." In *Structures*, vol. 33, pp. 1283-1298. Elsevier, 2021. https://doi.org/10.1016/j.istruc.2021.05.021
[20] Aktay, Levent, Alastair F. Johnson, and Bernd-H. Kröplin. "Combined FEM/meshfree SPH method for impact damage prediction of composite sandwich panels." (2005).
[21] Chang, Lijun, Shenglin Yuan, Xingyuan Huang, and Zhihua Cai. "Determination of Johnson-Cook damage model for 7xxx laminated aluminum alloy and simulation application." *Materials Today Communications* 34 (2023): 105224. https://doi.org/10.1016/j.mtcomm.2022.105224
[22] Lesuer, Donald R., G. J. Kay, and M. M. LeBlanc. *Modeling large-strain, high-rate deformation in metals*. No. UCRL-JC-134118. Lawrence Livermore National Lab.(LLNL), Livermore, CA (United States), 2001.
[23] Nassir, Nassier A., and Ayad K. Hassan. "Numerical response of aluminium plate (6061-T6) under dynamic loadings." In *IOP Conference Series: Materials Science and Engineering*, vol. 1076, no. 1, p. 012076. IOP Publishing, 2021. https://doi.org/10.1088/1757-899X/1076/1/012076
[24] Sanchidrian, Jose A., Ricardo Castedo, Lina M. Lopez, Pablo Segarra, and Anastasio P. Santos. "Determination of the JWL constants for ANFO and emulsion explosives from cylinder test data." *Central European journal of energetic materials* 12, no. 2 (2015): 177-194.
[25] IOLITEC, C. Properties, and T. Properties, "Technical data sheet Technical data sheet [C4MIM][NTf2]," *Cell*, vol. 123, no. May, pp. 98–99, 2005.
[26] Wei, Gang, Wei Zhang, Wei Huang, Nan Ye, Yubo Gao, and Yugang Ni. "Effect of strength and ductility on deformation and fracture of three kinds of aluminum alloys during Taylor tests." *International Journal of Impact Engineering* 73 (2014): 75-90. https://doi.org/10.1016/j.ijimpeng.2014.06.011
[27] Rakvåg, Knut Gaarder, Tore Børvik, Ida Westermann, and Odd Sture Hopperstad. "An experimental study on the deformation and fracture modes of steel projectiles during impact." *Materials & Design* 51 (2013): 242-256. https://doi.org/10.1016/j.matdes.2013.04.036